

is narrower for this material than for lanthanum tungsten bronze. Above  $x = 0.15$ ,  $\text{WO}_2$  appears. No yttrium tungstate structure<sup>2a,3</sup> could be detected even when the stoichiometric value of  $x$  was 0.2. Below  $x = 0.09$  a tetragonal form appears. It has the same lattice parameters as the tetragonal form of the lanthanum tungsten bronze. The cubic lattice parameter varies from 3.800 Å at  $x = 0.09$  to 3.815 Å at  $x = 0.15$ . Scandium does not form a tungsten bronze under the preparative conditions employed here. A mixture of  $\text{W}_{18}\text{O}_{49}$ <sup>4</sup> and  $\text{W}_{20}\text{O}_{58}$ <sup>5</sup> was found by X-ray examination.

Tungsten bronzes containing the rare earths have recently been described.<sup>6,7</sup> In the cases reported, a tetragonal form was found at low concentrations of the rare earths while at higher concentrations a cubic perovskite-type structure was found for all of the readily available rare earth elements. Magnetic studies<sup>8</sup> showed that the rare earth was present in a trivalent form. It would appear that both yttrium and lanthanum also form tungsten bronzes in their trivalent states. This is to be expected as these elements normally exist in a trivalent state and further have essentially the same radii as the rare earths in the 12-coordinated position of the perovskite lattice. Geller<sup>8</sup> has found that relative radii of  $\text{Y}^{3+}$ ,  $\text{Eu}^{3+}$ , and  $\text{La}^{3+}$  in the A position of perovskites to be 1.281, 1.304, and 1.346 Å, respectively. The cubic lattice parameters for the corresponding tungsten bronzes are in the same order.  $\text{Y}_{0.1}\text{WO}_3$  has a parameter of 3.802 Å and  $\text{Eu}_{0.1}\text{WO}_3$  was found to have a lattice constant of 3.815 Å<sup>6</sup> while  $\text{La}_{0.1}\text{WO}_3$  prepared here has a cubic parameter of 3.834 Å.

The color of  $\text{La}_x\text{WO}_3$  varies from green at  $x = 0.02$  to blue at  $x = 0.10$  and finally to red-purple at  $x = 0.19$ . A yellow form such as is found in the sodium tungsten bronzes at high sodium concentrations<sup>9</sup> does not appear here.

Electrical conductivity measurements on pressed powders of the materials synthesized here indicate that all the phases prepared, with the possible exception of  $\text{La}_{0.02}\text{WO}_3$ , have specific conductivities greater than 100 mhos/cm. The tungsten bronzes were not attacked by 3.7 *M* sulfuric acid at 90° even after 16 hr. The intense, lustrous color, the high electrical conductivity, the resistance to attack by acid, and the range of chemical composition of these materials characterize them as bronzes.<sup>10</sup>

**Acknowledgment.**—We wish to thank the U. S. Army Electronics Command, Fort Monmouth, N. J., for supporting this research under Contract DA 36-039 AMC-03743(E). The author is indebted to Professor E. Banks for many stimulating discussions, to Mr. J. T.

Allen, Jr., for his aid in obtaining the X-ray data, and to Mr. J. T. Pavlovcak for his help in preparing the materials.

CONTRIBUTION FROM THE RESEARCH LABORATORIES,  
XEROX CORPORATION, ROCHESTER, NEW YORK 14603

## The Crystal Structure of Trigonal Selenium<sup>1</sup>

BY PAUL CHERIN AND PHYLLIS UNGER

Received January 31, 1967

Because of the intensified interest in trigonal selenium in recent years, an investigation of the Se-Se bond length, bond angle, and interchain separation was undertaken, using modern techniques of collecting and analyzing data. Elemental selenium can exist in several solid modifications: two monoclinic ( $\alpha$  and  $\beta$ ), a trigonal, a vitreous, and a cubic modification. Under normal conditions of temperature and pressure, only the trigonal phase is stable; the others, being metastable, slowly convert to the trigonal form. A previous crystal structure determination of trigonal selenium was completed by Bradley,<sup>2</sup> who used powder photography techniques.

### Experimental Section

Crystals were grown by slowly cooling a saturated solution of amorphous selenium in hot aniline. The resulting needle crystals were mounted parallel to their long axis, which was parallel to the  $c$  axis of the hexagonal cell. Those which were relatively strain free and with regular hexagonal cross sections (diameters were about 0.2 mm) were selected for further study. Two-dimensional  $hk0$  data were collected using a General Electric XRD-5 unit equipped with a quarter-circle Eulerian cradle goniostat, a scintillation counter, and a pulse-height discriminator. Both  $\text{Cu K}\alpha$  and  $\text{Mo K}\alpha$  radiation (filtered with Ni and Zr, respectively) were used.

### Determination and Structure

The stationary crystal-stationary counter method was used to record the reflections. This was related to integrated intensity in the usual manner.<sup>3</sup> Difficulties were encountered owing to high and rapidly changing background.

For convenience, the unit cell is generally treated as hexagonal. The hexagonal cell dimensions, determined by Swanson, Gilfrich, and Ugrinic,<sup>4</sup> are  $a = 4.3662$  and  $c = 4.9536$  Å. The space group is either  $P3_121$  or  $P3_221$ . There are three atoms per unit cell, lying on twofold axes; the position of the asymmetric atom in the hexagonal cell can be described by one parameter. The usual Lorentz and polarization corrections were made. An absorption correction was

(3) K. Nassau, H. J. Levinstein, and G. M. Loiacono, *J. Phys. Chem. Solids*, **26**, 1805 (1965).

(4) ASTM X-Ray Powder Diffraction Cards 5-0392 and 5-0393.

(5) ASTM X-Ray Powder Diffraction Cards 5-0386 and 5-0387.

(6) W. Ostertag, *Inorg. Chem.*, **5**, 758 (1966).

(7) C. V. Collins and W. Ostertag, *J. Am. Chem. Soc.*, **88**, 3171 (1966).

(8) S. Geller, *Acta Cryst.*, **10**, 248 (1957).

(9) M. J. Sienko, *Advances in Chemistry Series*, No. 39, American Chemical Society, Washington, D. C., 1963, paper 21.

(10) S. Anderson and A. D. Wadsley, *Acta Cryst.*, **16**, 201 (1962).

(1) Presented at the 7th International Congress and Symposium of the International Union of Crystallography, Moscow, July 12-21, 1966.

(2) A. J. Bradley, *Phil. Mag.*, **48**, 477 (1924).

(3) L. E. Alexander and G. S. Smith, *Acta Cryst.*, **15**, 983 (1962).

(4) H. E. Swanson, N. T. Gilfrich, and G. M. Ugrinic, National Bureau of Standards Circular 539, Vol. 5, U. S. Government Printing Office, Washington, D. C., 1955, p 54.

applied to the data, based on the assumption that the crystals were cylindrical. Although this was a source of error, a complete set of equivalent reflections was measured and averaged in each case, tending to reduce the error. Near the end of the refinement the diameter of the "cylinder" was permitted to vary. The position parameter, the standard deviation, and the reliability factor were found to be rather independent of small changes in the assumed diameter.

An anomalous dispersion correction was necessary because selenium shows considerable anomalous scattering when irradiated with Cu  $K\alpha$  and Mo  $K\alpha$ . Fortunately, in the case of a chemical element, it is possible to apply a dispersion correction directly to the observed structure factors and avoid the involved corrections described by Patterson<sup>5</sup> and Ibers and Hamilton.<sup>6</sup> For any unit cell containing one kind of atom, one may write

$$|F_{\text{cor}}| = |F_o| / [(1 + \delta_1)^2 + \delta_2^2]^{1/2} = [A^2 + B^2]^{1/2}$$

where  $A = f_o H$ ,  $B = f_o K$ ,  $\delta_1 = \Delta f' / f_o$ , and  $\delta_2 = \Delta f'' / f_o$ , and  $H$  and  $K$  are geometrical structure factors and include the temperature factors. The observed structure amplitude may now be corrected for dispersion and used directly in a least-squares refinement. For a Fourier summation, the phase angle,  $\phi$ , is determined in the usual way, *i.e.*,  $\tan \phi = B/A$ .

Since so few parameters were to be determined, a least-squares refinement was applied directly, using a program written by Busing, Martin, and Levy (ORFLS)<sup>7</sup> starting with the positional parameter of  $x = 0.217$  reported by Bradley. The function minimized was  $\Sigma w(|F_o| - |F_c|)^2 / \Sigma w F_o^2$ , where  $w$ , the weighting factors, were taken from Evans<sup>8</sup>

$$w(hkl) = 1/\sigma^2(hkl)$$

$$\sigma(hkl) = 1/2[c(P + Q)/(P - Q)]^{1/2}$$

where  $\sigma(hkl)$  is the standard deviation of the  $hkl$  reflection,  $c$  contains the geometrical factors such as Lorentz and polarization corrections,  $P$  is the total number of counts recorded for a reflection, and  $Q$  is the number of background counts.

Both copper and molybdenum data were refined in four cycles. Later, both sets of data were combined and once more refined.

### Results

The position and thermal parameters are given in Table I. This table also includes the appropriate bond length and angle as well as the root-mean-square vibrational amplitude of motion in the  $aa$  plane. In spite of the small number of independent reflections, the position parameter seemed relatively independent of the weighting. Two other weighting schemes were

TABLE I  
THERMAL AND POSITION PARAMETERS  
OF TRIGONAL SELENIUM

	Cherin and Unger (1966)	Bradley (1924)
$x$	$0.2254 \pm 0.0010$	0.217
Bond length, A	$2.373 \pm 0.005$	2.33
Bond angle, deg	$103.1 \pm 0.2$	104.8
$\beta_{11}$	$0.0338 \pm 0.0020$	
$\beta_{22}$	$0.0417 \pm 0.0043$	
Rms vibrational amplitude (along "a"), A	$0.174 \pm 0.006$	
Rms vibrational amplitude (perpendicular to "a"), A	$0.150 \pm 0.004$	
$R$ , %	3.2	

used, and the position parameter did not change by more than one standard deviation.

The observed and calculated structure amplitudes are given in Table II. Ten reflections were observed with Cu  $K\alpha$  radiation and Mo  $K\alpha$  yielded an additional two. The intensities decreased very sharply in the range  $50$ – $60^\circ$ ,  $2\theta$  (Mo  $K\alpha$ ). A great deal of scattering in the radial direction was observed on our Weissenberg photographs. These effects were attributed to defects in the structure.

TABLE II  
OBSERVED STRUCTURE AMPLITUDES FOR TRIGONAL SELENIUM

$hkl$	$F_o$	$F_c$
100	109.3	113.33
200	60.0	60.25
400	69.9	74.39
500	38.9	39.69
110	125.4	123.68
220	57.7	57.19
330	37.3	39.71
120	124.8	123.80
130	29.8	25.15
230	33.2	33.28
140	35.5	34.85
240	16.3	15.57

The Se–Se bond length is somewhat longer than the value reported by Bradley,<sup>2</sup> and it is also longer than the average Se–Se bond length of  $2.34 \pm 0.02$  A reported by Burbank<sup>9</sup> for  $\alpha$ -Se, a monoclinic phase in which the atoms bond in ring form. The bond angle we have found in trigonal selenium is in good agreement with the value of  $102.6^\circ$  reported for trigonal tellurium.

Only two temperature coefficients needed to be determined because of the restrictions imposed by the twofold axis in the hexagonal cell. Of course,  $b_{33}$ ,  $b_{13}$ , and  $b_{23}$  could not be determined from  $hk0$  data. The values determined for the root-mean-square amplitudes of vibration indicate the motion is rather isotropic in the  $aa$  plane. No attempt has been made to separate these amplitudes into interatomic vibration and chain motion, nor has any attempt been made to correct the bond length for any "riding" motion that might exist. A recent study of tellurium has just been completed. The calculated root-mean-square amplitudes of vibration are almost identical with the corresponding selenium parameters.

(5) A. L. Patterson, *Acta Cryst.*, **16**, 1255 (1963).

(6) J. A. Ibers and W. C. Hamilton, *ibid.*, **17**, 781 (1964).

(7) W. R. Busing, K. O. Martin, and H. A. Levy, "A Crystallographic Least-Squares Refinement Program for the IBM 704," ORNL-59-4-37, 1959.

(8) H. T. Evans, Jr., *Acta Cryst.*, **14**, 689 (1961).

(9) R. D. Burbank, *ibid.*, **4**, 140 (1951).

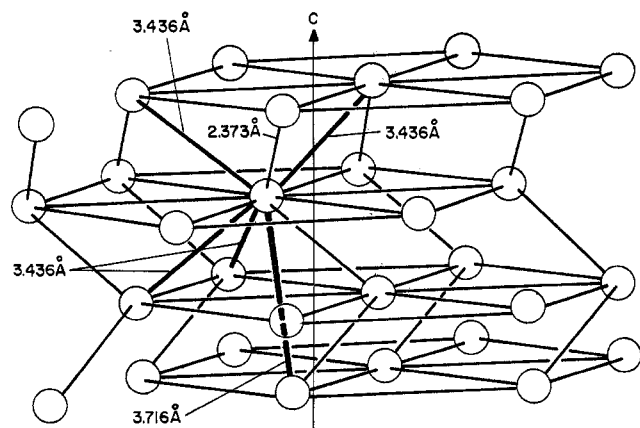


Figure 1.—Nearest neighbor distances in trigonal selenium.

Several important coordination distances are given in Figure 1. The nearest neighbor distance of atoms on adjacent chains (3.436 Å) is considerably shorter than the 4.0 Å one would expect if only van der Waals forces were operating between the chains.<sup>10</sup>

The reliability factor

$$R = \frac{\sum_n^N \frac{|F_o - |F_c||_n}{\sum_n^N |F_o|_n}$$

where  $N$  is the total number of observed reflections, for the combined data is quite good. However, with so few independent variables and data points (only 12 independent reflections were observed with Mo  $K\alpha$  radiation; see Table II), the standard deviations for each parameter (Table I) should be more indicative of the precision of this work.

Investigation of three-dimensional data is planned in order to learn more about the defect structure of the vibrational motion of the chains.

(10) A. Von Hippel, *J. Chem. Phys.*, **16**, 372 (1948).

CONTRIBUTION FROM THE DEPARTMENT OF CHEMISTRY,  
MICHIGAN STATE UNIVERSITY, EAST LANSING, MICHIGAN 48823

## The Infrared Spectra of Transition Metal Complexes of Pentamethylenetetrazole<sup>1</sup>

BY FRANK M. D'ITRI AND ALEXANDER I. POPOV

Received February 4, 1967

In our previous communications<sup>2</sup> we described the preparation and physical properties of three types of transition metal perchlorate complexes of pentamethylenetetrazole (hereafter abbreviated at PMT) having the

(1) Taken in part from the M.S. thesis of F. M. D'Itri, Michigan State University, Feb 1966.

(2) (a) H. A. Kuska, F. M. D'Itri, and A. I. Popov, *Inorg. Chem.*, **5**, 1272 (1966); (b) F. M. D'Itri and A. I. Popov, *ibid.*, **5**, 1670 (1966); (c) F. M. D'Itri and A. I. Popov, *ibid.*, **6**, 597 (1967).

compositions:  $\text{Cu(PMT)}_2\text{ClO}_4$ ,  $\text{Cu(PMT)}_4(\text{ClO}_4)_2$ , and  $\text{M}^{\text{II}}(\text{PMT})_6(\text{ClO}_4)_2$ , where  $\text{M}^{\text{II}} =$  manganese(II), iron(II), cobalt(II), nickel(II), copper(II), or zinc(II). Physicochemical measurements indicate that the hexacoordinated transition metal complexes are isomorphous and have octahedral configurations.

The present work was undertaken to determine the infrared spectra of these complexes in the 5000–180- $\text{cm}^{-1}$  spectral region so as to obtain some information on the structure of these compounds and the nature of the metal–ligand bond.

### Experimental Section

The materials, preparation, description, analytical data, and physicochemical properties of the transition metal complexes of PMT of the type  $\text{M}^{\text{II}}(\text{PMT})_6(\text{ClO}_4)_2$ ,  $\text{Cu(PMT)}_4(\text{ClO}_4)_2$ , and  $\text{Cu(PMT)}_2\text{ClO}_4$  have been described in previous publications.<sup>2</sup>

**Infrared Measurements.**—Infrared spectra in the 5000–670- $\text{cm}^{-1}$  spectral regions were obtained on a Beckman IR-5A spectrometer. The solid complexes were dispersed in Nujol. An attempt was made to measure the spectra of complexes in KBr pellets, but the compounds appeared to undergo a partial decomposition in the KBr press with the formation of metal-bromide complexes.

The measurements in the 670–180- $\text{cm}^{-1}$  regions were carried out on a Perkin-Elmer 301 spectrometer. All of the spectra were obtained on Nujol mulls which were supported between plates of cesium bromide or polyethylene windows and using air or polyethylene of the same thickness as references. The entire system was continually flushed with dry nitrogen.

In order to obtain spectra of the complexes in the 700–100- $\text{cm}^{-1}$  region, it was necessary to change gratings, mirrors, choppers, and reststrahlen filters several times. It was, therefore, found convenient to obtain the spectra of all of the compounds under investigation in one region before modifying the instrument for the next region. For this reason, the relative intensities of bands for the same sample in different regions probably do not have much significance. The breaks in the spectra due to these changes are shown on the figures by interruptions in the traces.

The stabilities of the complexes in the Nujol mulls were checked by remeasuring some of the spectra after 24 hr. In all cases the spectra were reproducible.

### Discussion and Results

(1) **Infrared Spectra in the 5000–670- $\text{cm}^{-1}$  Region. Hexakis(pentamethylenetetrazole)–Transition Metal–Perchlorate Complexes.**—The comparison of the spectrum of PMT with those of the hexakis(pentamethylenetetrazole)–transition metal–perchlorate complexes shows little change in the PMT spectrum upon complexation. There are, however, small ( $\pm 3\text{-cm}^{-1}$ ) absorption shifts which vary with the respective central metal ion. The uncomplexed perchlorate ion has a regular tetrahedral structure and belongs to the point group  $T_d$ .<sup>3</sup> If, in the process of complexation, the  $\text{ClO}_4^-$  ion becomes coordinated to the metal ion, the oxygen atom involved in the partial covalent bonding is no longer equivalent to the other three oxygen atoms, and the symmetry of the perchlorate group is lowered to  $C_{3v}$ . As a result, the broad, degenerate  $\nu_3$  band splits into two well-defined bands with maxima between 1200 and 1000  $\text{cm}^{-1}$ . Likewise, the chlorine-coordinated oxygen ( $\text{Cl}-\text{O}^*$ ) stretching frequency  $\nu_2$

(3) B. J. Hathaway and A. E. Underhill, *J. Chem. Soc.*, 3091 (1961).